Environment Protection Engineering

Vol. 46 2020 No. 4

DOI:10.37190/epe200402

KAI XU[1], JIAHAO WANG[1], JIACHENG LI[1], ZIJIE WANG[1], ZIZENG LIN[1], ZHENG WANG[1]

ATTAPULGITE SUSPENSION FILTER MATERIAL FOR BIOLOGICAL AERATED FILTER TO REMOVE COD_{Mn} AND AMMONIA NITROGEN IN MICROPOLLUTED DRINKING WATER SOURCE

An attapulgite suspended (AS) filter material was successfully prepared and used in combination with biological aerated filter (BAF) to pretreat excess organic matter and ammonia nitrogen in micropolluted water. The AS filter material was of low density and floated on the water surface, which is beneficial to optimize the hydraulic conditions. Through scanning electron microscopy (SEM) and Fourier transform infrared spectroscopy (FTIR) It was found that the surface of the filter material was uneven, the pores were deep. When the hydraulic load is 4 m/h and the gas to water volume ratio is 2:1, the removal rates of permanganate index (COD_{Mn}) and ammonia nitrogen by ASBAF are up to 57.49 and 88.11%, respectively, and the effluent quality meets relevant standards. After backwashing, the pollutants removal rate will return to stable filtration after two hours. A short-term shutdown of the reactor has little effect on the processing performance of ASBAF, but a long-term shutdown will greatly affect the removal rate of COD_{Mn}. The complete organic matter degradation model can well fit the experimental effluent water quality.

1. INTRODUCTION

Since the outbreak of the 2019-nCoV, more and more people have begun to pay attention to public health safety. The researchers isolated live new coronavirus in stool samples from patients with severe coronavirus pneumonia, suggesting that there may be a new route for the spread of the new coronavirus [1]. Therefore, the pretreatment of drinking water is particularly important.

Micropolluted water refers to the drinking source water that some of the projects slightly exceed the prescribed standards for Class III water bodies in the Surface Water Environmental Quality Standard (GB3838-2002) of China. Projects that exceed the

[1]School of Civil Engineering, Nanjing Forestry University, Nanjing 210037, P.R. China, corresponding author Zheng Wang, email address: wangzheng@njfu.edu.cn

standard usually include organic matter, ammonia nitrogen, suspended solids and inorganic substances. For example, when the permanganate index (COD_{Mn}) exceeds 6 mg/dm^3 or the concentration of ammonia nitrogen exceeds 1.0 mg/dm^3, and other projects meet the standard, the source water is micropolluted water. The source of pollution of micropolluted water is the waste derived from industrial, agricultural and domestic discharges. Besides, antibiotic resistant bacteria are not only present in Poland's water supply system [2] but also found in China's drinking water system [3].

The construction of constructed wetlands through plants, substrates [4, 5], and microbial-fuel-cells-coupled [6] can purify water well but requires superimposed processing time. A biological aerated filter (BAF) is a form of the biological contact oxidation technology that is widely applied for the treatment of actual wastewater. Different filter media can enhance the removal performance of various contaminants. The function of a simultaneous nitrification and denitrification (SND) reactor can be enhanced by using non-uniform filter media [7]. BAF is rarely used as a drinking water treatment unit but is used to treat excessive ammonia in raw water in water purification plants. BAF needs to be improved when it is used as a drinking water pretreatment unit, and the filter material can be optimized [8].

Attapulgite has a large specific surface area, high viscosity, and contains a large number of silanol groups and exchangeable ions. It can be used as a water treatment adsorption material with low cost and excellent adsorption performance [8]. The attapulgite activated carbon composite filter BAF has considerable potential for removing dibutyl phthalate (DBP) from drinking water [9].

To treat the micropolluted water into a qualified drinking source water, a biological aerated filter with attapulgite suspended filter material (ASBAF) has been built to remove excess COD_{Mn} and ammonia nitrogen in the micropolluted water. If the micropolluted water becomes qualified source water after ASBAF treatment, then it can be proved that ASBAF has a certain removal effect on COD_{Mn} and ammonia nitrogen in the micropolluted water. The study conducted in this research includes (1) preparation of an attapulgite suspended filter (AS) and application to BAF, (2) pretreatment of micropolluted water with ASBAF to make it a qualified drinking source water, (3) effect of operating conditions on the performance of ASBAF, and (4) estimation of the effluent quality under certain conditions by established an organic matter degradation kinetics model.

2. MATERIALS AND METHODS

Materials. The primary chemicals were all pure and of analytical grade, and deionized water was used. All chemicals were purchased from Nanjing Chemical Reagent Co., Ltd. The raw materials related to the preparation of AS were provided by Anhui Huasheng Environmental Protection Technology Co., Ltd., China.

The raw water tested was artificially prepared by adding to deionized water such compounds as ammonium chloride (18.09 mg/dm^3), glucose (12.50 mg/dm^3), potassium dihydrogen phosphate (0.67 mg/dm^3), ferrous chloride (0.22 mg/dm^3), cobalt chloride hexahydrate (0.27 mg/dm^3), manganese sulfate heptahydrate (0.021 mg/dm^3), zinc chloride (0.10 mg/dm^3), ammonium molybdate tetrahydrate (0.023 mg/dm^3), copper sulfate pentahydrate (0.093 mg/dm^3) and calcium chloride (0.045 mg/dm^3). The specific water quality indicators are given in Table 1.

Table 1

Raw water quality

Index	Range of values
pH	6.54–7.87
Temperature, °C	25.3–28.9
COD_{Mn}, mg/dm^3	6.18–9.14
NH_4^+-N in mg/dm^3	2.97–6.90

Preparation of AS. The sifted and dried feldspar, basalt, fly ash, bentonite, fluorite powder, sodium hydrogen carbonate, and magnesium carbonate were mixed, and then distilled water was added to prepare a slurry in the following proportion 10:40: 10:1:1:19:19:19:19:33. The mixture was granulated (Purui, QJ-500, China) and dried in an oven (Boxun, GZX-9140MBE, China) at 105–110 °C for 4 h. Then, it was preheated in a muffle furnace (Tester, SX-12-10, China) at 700 °C for 0.5 h, and quickly transferred to an electric furnace (Tianyouli, SKQ-6, China) to continue calcination at 800 °C for 1.5 h. After cooling to room temperature, a semi-finished product was obtained which was mixed with attapulgite in a weight ratio of 2:1, and then placed in a sugar-coating machine (Wugang, BY-500, China, 25–35 rpm, a disc tilt of 40–50°) for 0.5 h to form balls of a spherical shape. A 2% aqueous solution of BP-17 PVA was sprayed during the formation of the ball. Then, the product was allowed to stand for 1 h naturally dried for 3 h. Finally, it was dried in an oven (Boxun, GZX-9140MBE, China) at 105 –110 °C for 4 h to obtain AS. Figure 1 shows the photograph of AS.

Methods of characteristics. The microstructure of the AS filter was observed by SEM (FEI, Quanta 200, U.S.A.). The AS filter materials were crushed and dried and adhered to the copper mesh. Since the filter material had poor conductivity, the conductive layer must be evaporated, and the copper mesh was placed in the SEM to observe and receive an image.

The functional groups on AS were analyzed by Fourier transform infrared spectroscopy (FTIR) (Thermo Scientific, Nicolet Iis 5, U.S.A.). A small amount of dried AS was ground into a powder, and then potassium bromide and AS powder were mixed in a mass ratio of 300:1 to prepare a sample. The scanning wave number ranges from 15 500 to 10 cm^{-1} with a resolution of 0.2 cm^{-1}.

Description of the ASBAF system and experimental methods. The dynamic experimental device (Fig. 1) consisted of a cylindrical plexiglass column, 3 m high and 10 cm in diameter. The thickness of the filter material was 120 cm. The gas used in ASBAF was air. Four gas to water volume ratios of 0.5:1, 1:1, 2:1, and 3:1 were used to study the effect on the performance of ASBAF, under the conditions of the hydraulic load of 4 m/h and hydraulic retention time of 0.3 h. Each working condition run for 4 days.

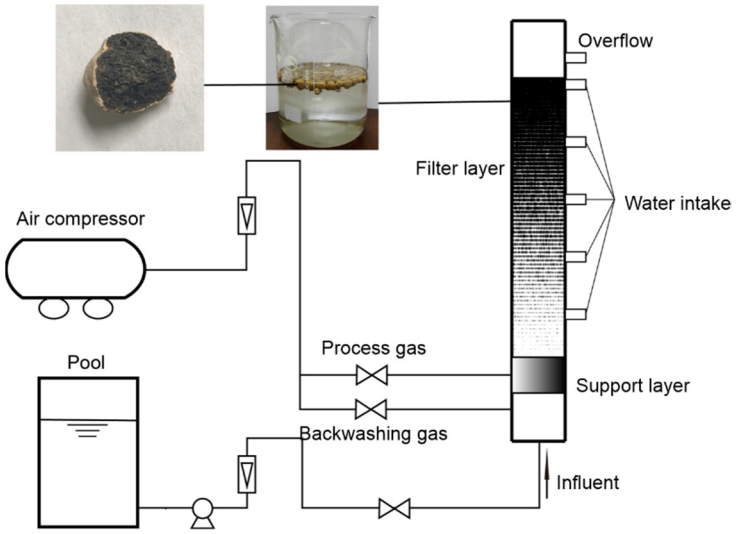

Fig. 1. Photograph of AS and experimental schematic of ASBAF

The hydraulic load was adjusted mainly by adjusting the influent flow. Under the condition of 2:1 gas to water volume ratio, the influent hydraulic loads were 1.4, 2.0, 3.0, 4.0, 5.0, 6.0, 7.0 m/h, respectively. Under the established conditions, the device worked for 2 days.

The concentrations of organic matter and ammonia nitrogen were changed by changing the amount of glucose and ammonium chloride added to the raw water. The performance of ASBAF on COD_{Mn} load resistance and ammonia nitrogen load resistance were investigated. Under the condition of the hydraulic load of 4.0 m/h and gas to water ratio of 2:1, the COD_{Mn} concentration of organic matter was changed from 4.23 to 18.04 mg/dm^3 and the ammonia nitrogen concentration was changed from 2.34 to 18.73 mg/dm^3.

Under the condition of a hydraulic load of 4.0 m/h and gas to water ratio of 2:1, a total of five outlets were provided at the heights of 40, 60, 80, 100, and 120 cm of the filter column. From the sampling and analysis of the five outlets, the removal effect of COD_{Mn} and ammonia nitrogen on the height of the ASBAF filter layer was studied.

The backwashing method selects the air-water backwashing. The operating conditions of ASBAF before and after backwashing were a hydraulic load of 4 m/h, a gas to water ratio of 2:1, an influent COD_{Mn} concentration of 8.38 mg/dm^3, and an influent

ammonia nitrogen concentration of 3.61 mg/dm^3. The backwashing conditions were a hydraulic load of 10 m/h, and a gas to water ratio of 5:1. The hydraulic load and gas to water ratio of the backwashing were kept constant. Sampling was carried out 2 h before backwashing and 2, 4, 6, 8, and 10 h after backwashing to investigate the effect of ASBAF on the removal of COD_{Mn} and ammonia nitrogen after backwashing.

To study the effect of closing time on the recovery performance of ASBAF, three experiments were conducted. The closing time of each experiment was three days, seven days and fifteen days. Before and after each closing, the ASBAF was operated at a hydraulic load of 4 m/h and gas to water ratio of 2:1. After the reactor's removal rates of COD_{Mn} and ammonia nitrogen had stabilized for one week, the reactor was closed for the next test. Before the filter was started, the ASBAF was backwashed. After the start of the operation, water samples were taken at 2, 4, 6, 8, 10, 14, and 20 h for analysis.

In this experiment, the natural membrane method was adopted. The biofilm was considered to form when the COD_{Mn} removal rate is stable at about 25% and the ammonia nitrogen removal rate was stable at about 65%. Each change of operating condition required biomass adaptation time to reach a new equilibrium state. Therefore, in this paper, all tests were conducted after 24 h of each change of operating condition.

Methods of analysis. The effluent samples were collected in 1 dm^3 polypropylene bottles and immediately analyzed. Excess mixed liquid suspension solids (MLSS) were filtered using an organic filter of 0.45 μm pore size. The COD_{Mn} was measured by the acid method according to the water and wastewater detection and analysis method [10]. The ammonium nitrogen (NH_4^+-N) was determined spectrophotometrically (at 425 nm) using an ultraviolet spectrophotometer [10].

Kinetics model of ASBAF organic matter degradation. The organic matter degradation model was based on the Monod equation (Fig. 2). Before deriving the matrix degradation kinetics model, the following assumptions were made: (1) the ABSAF reactor is an ideal push-flow reactor; (2) the biofilm is a steady-state active organism growth and death is a dynamic equilibrium relationship, homogeneous organism, the density and thickness are consistent and the same; (3) the reaction kinetic parameters are consistent in the solution and the biofilm, and the distribution of pH and temperature in the reactor remain unchanged; (4) the degradable matrix in the reactor exists in a dissolved state. The degradation of the matrix is caused by the biofilm, and the suspended biomass in the solution does not participate in the degradation process of the matrix.

The Monod equation has the form of [11].

$$\mu = \mu_{\max} \frac{S}{K_s + S} \tag{1}$$

where μ is a specific growth rate of microorganisms, i.e., the rate of proliferation of unit biomass, S is the concentration of organic substrate, K_s is a saturation constant corresponding to the substrate concentration at $\mu = 0.5\mu_{max}$.

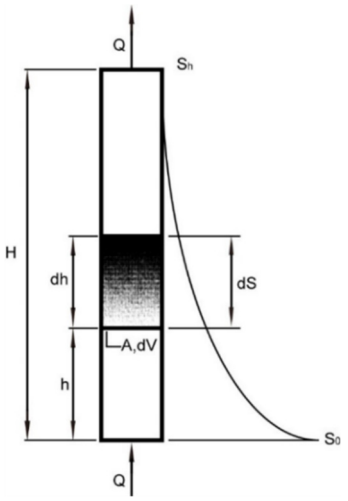

Fig. 2. Schematic diagram of the organic matter degradation model

In water treatment, microbial specific degradation rate v is

$$v = \lambda\mu \tag{2}$$

where μ is the ratio of the specific degradation rate of the organic substrate to the specific growth rate of the microorganism, λ a coefficient.

After substituting equation (2) into (3) we have

$$v = v_{max}\frac{S}{K_s + S} \tag{3}$$

where v_{max} was the maximum specific degradation rate of an organic substrate.

The specific degradation rate following its definition is

$$v = -\frac{dS}{Mdt} = \frac{S_0 - S}{Mdt} \tag{4}$$

where S_0, S are the initial and actual concentrations of organic substrate in water, M – the total amount of active organisms in the reactor.

Thus we arrive at the degradation rate of organic substrate V_t

$$V_t = -\frac{dS}{dt} = v_{max}\frac{MS}{K_s + S} \tag{5}$$

When the influent organic matter concentration is low, $S \ll K_s$ [12] (active biomass in ASBAF is mainly in the biofilm and is homogeneously stable) and equation (5) takes the form of

$$V_t = \frac{dS}{dt} = -KS \tag{6}$$

where V_t is the reaction rate, $K = v_{max}(M/S)$ the rate constant relating to specific reaction time, substrate concentration, reaction environment, active biomass.

In the ideal form of BAF reactor, the biofilm distribution is uniform and mass transfer occurs only in the lateral direction. The following balance related to organic matter (OM) exists in each local microelement per unit time OM input – OM output – OM removal quantity = OM cumulative amount [13]:

$$QdS - v_1 Adh - v_2 Adh = \frac{dS}{dh} Adh \tag{7}$$

where Q is the amount of water treated, dS – organic matter concentration in the microelement, v_1 – degradation efficiency of organic matter by microorganisms in biofilm, v_2 – degradation efficiency of organic matter in by suspended microorganisms in a microelement, A – cross-section area of a filter microelement, dh – a microelement height, $\frac{dS}{dh}$ – rate of organic matter concentration in a microelement.

For steady-state biofilms, there is no accumulation of organic matter in the microelement, so $\frac{dS}{dh} Adh = 0$. The active biomass is mainly present in the biofilm, and the suspended biomass is negligible, so $v_2 = 0$. Thus, we obtain

$$QdS = v_1 Adh \tag{8}$$

The degradation of organic matter occurring in the ASBAF reactor is of the first order. From equation (6) we have

$$\frac{dS}{S} = -\frac{KA}{Q} dh \tag{9}$$

When $h = 0$, $S = S_0$, by solving equation (9) we arrive at

$$S = S_0 \exp\left(-\frac{KA}{Q} h\right) \tag{10}$$

where S is the concentration of organic matter at the height of h when ASBAF is stable, S_0 the influent organic matter concentration, A – effective cross-section area of the filter, h – filter height.

The purpose of this research was to construct a BAF process that can treat micropolluted water into a qualified drinking source water. In this study, we evaluated the potential of ASBAF on the treatment of micropolluted water and established a kinetics model of ASBAF organic matter degradation.

3. RESULTS AND DISCUSSION

3.1. CHARACTERISTICS OF AS

The suspended filter material is a thin layer of attapulgite wrapped around the core with a yellowish color, rough surface, upon which bacteria are easily attached and promotes rapid biofilm formation (Fig. 3).

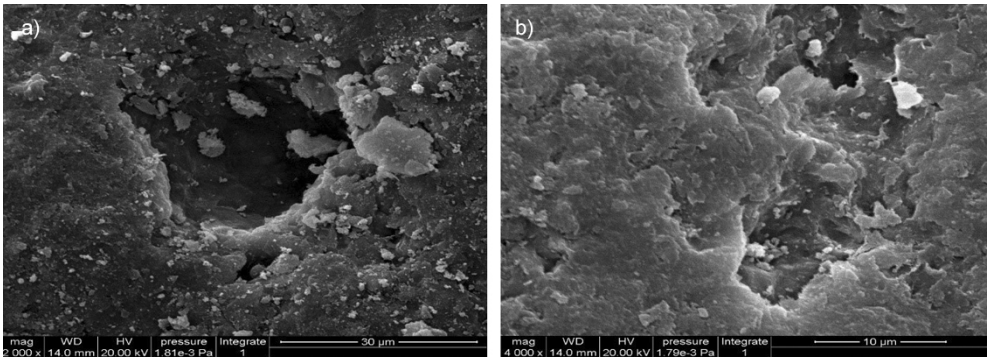

Fig. 3. SEM image of AS at magnification 2000× (a), and 4000× (b)

The surface of the filter material is uneven, has deep pores and many non-connected honeycomb micropores. This is because of the addition of the foaming agents – magnesium carbonate and ammonium hydrogen carbonate, which results in a density close to that of water. The reactor was equipped with a layer of plastic mesh, which can retain AS in the reactor. All the AS filter materials were suspended below the liquid level, and the amounts of ASs were proportional to the layer height.

The AS filter material has a few infrared spectrum absorption peaks (Fig. 4). The strongest absorption peak at 1029.84 cm^{-1} corresponds to stretching vibration Si–O. The AS filter material has a high silica content with other less abundant compounds. The absorption peak at 1438.12 cm^{-1}, attributed to $–CH_2–$, is the second strongest one, indicating that the AS filter material contains a large amount of methylene; at 473.34 cm^{-1}, we have

the Mg–O vibration, which indicates that magnesium oxide is present in the AS material. –OH stretching vibrations at 3430.97 cm^{-1} of the crystal water are also present.

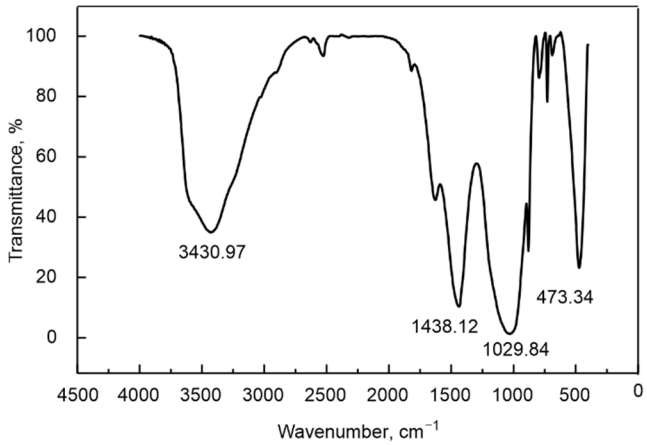

Fig. 4. FTIR spectra of AS

3.2. EFFECT OF GAS TO WATER RATIOS ON THE REMOVAL OF COD_{Mn} AND AMMONIA NITROGEN BY ASBAF

Adjusting the gas to water ratio has an important effect on the DO concentration at different heights. Within a certain range, the concentration of dissolved oxygen in water is positively correlated with the gas to water ratio [14]. The optimal biofilm thickness and various microbial species differ depending on the DO levels, and the optimal DO concentration can enhance the microbial community structure [15]. Figure 5a illustrates that when the remaining operating conditions are unchanged, and the gas to water ratio increases from 0.5:1 to 2:1, the removal rates of COD_{Mn} and ammonia nitrogen increase to 37.68 and 78.07%, respectively. The initial gas to water ratio of 0.5:1 resulted in a lower DO concentration in the system, and the average removal rates of COD_{Mn} and ammonia nitrogen were only 29.44 and 68.62%, which indicates that a low gas to water ratio does not provide enough DO. The heterotrophic bacteria that remove COD_{Mn} and the nitrifying bacteria that nitrated NH_4^+-N are all aerobic bacteria, so the lower DO concentration has a stronger inhibitory effect on the activities of heterotrophic bacteria and nitrifying bacteria, resulting in low removal rate of pollutants [16]. When the gas to water ratio is 2:1, the average removal rates of COD_{Mn} and ammonia nitrogen are optimal under the conditions of a hydraulic load of 4 m/h. COD_{Mn} and NH_4^+-N are effectively removed in respective advantageous treatment environments because of changes in DO concentration [17, 18]. Currently, the DO concentration in the system is high, which is

beneficial to the growth and reproduction of heterotrophic bacteria and nitrifying bacteria, and improves the degradation rate of COD_{Mn} and NH_4^+-N. In addition, when the hydraulic load conditions are not changed, that is, the organic matter concentration and the hydraulic retention time are substantially unchanged, increasing the gas to water ratio can increase the turbulent conditions of the water flow, improve the mass transfer conditions of the filter material, and strengthen the biochemical reaction, further reducing the concentration of the pollutants [8].

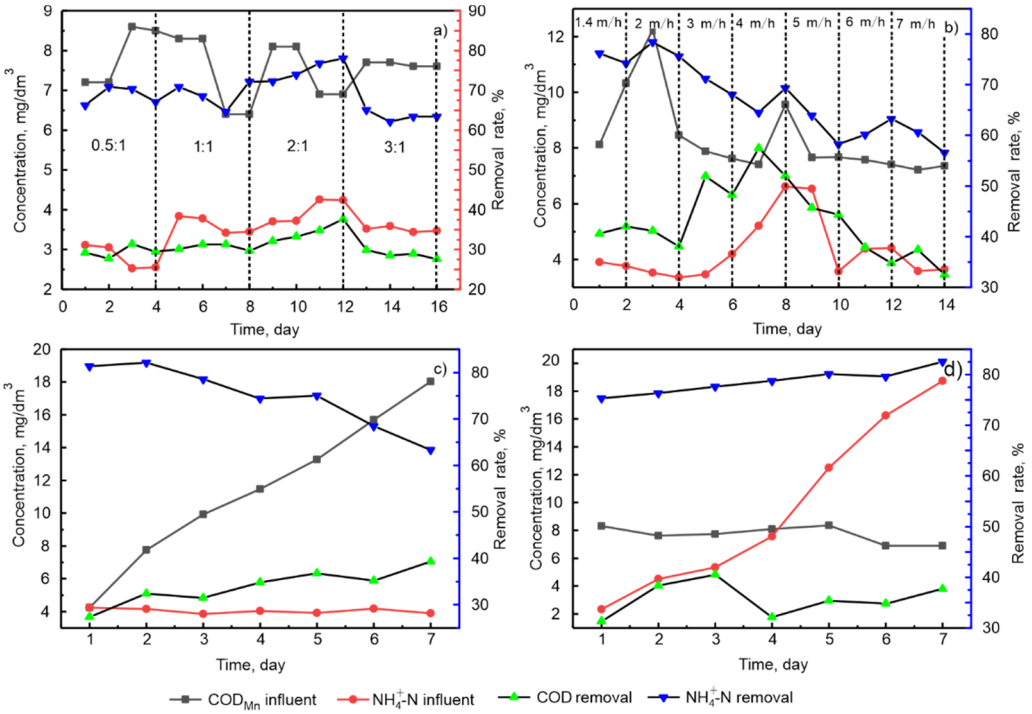

Fig. 5. Time dependences of load concentration for various gas to water ratios (a), hydraulic loads (b), organic impact loads (c), and ammonia nitrogen (d)

When the gas to water ratio increased from 2:1 to 3:1, the removal rates of COD_{Mn} and ammonia nitrogen decreased to different degrees. The average removal rates of COD_{Mn} and ammonia nitrogen were only 28.76 and 63.49%. The DO in the water has a certain saturation concentration. The gas to water ratio is too large, resulting in the DO in the water to resolve and inhibit the activity of the microorganism. Excessive gas to water ratio also enhances the scouring effect of the biofilm, resulting in a large shear force that enhances the removal of biofilms from the filler wall. Biofilm detachment not only reduces the removal rate of pollutants, but also the biofilm that has fallen off causes the effluent COD_{Mn} to be high, resulting in poor effluent quality [19].

3.3. EFFECT OF HYDRAULIC LOAD ON THE REMOVAL OF COD_{Mn} AND AMMONIA NITROGEN BY ASBAF

The performance of BAF varies with different hydraulic load [19]. Figure 5b illustrates that the removal rate of COD_{Mn} increases first and then decreases with the increase of hydraulic load, and the removal rate of ammonia nitrogen decreases with the increase of hydraulic load. When the hydraulic load increased from 1.4 to 4 m/h, the average removal rate of COD_{Mn} increased from 41.32 to 54.74%, and the average removal rate of ammonia nitrogen decreased from 75.21 to 66.91%. Increasing the hydraulic load can make the matrix and biomass in the filter more evenly distributed and promote the mass transfer process between the liquid phase and the biological phase. The nutrients available to the microorganisms are correspondingly increased so that the microbial growth rate is increased, the degradation activity is sufficient, and the removal rate of COD_{Mn} improved. When the hydraulic load increases, influent flow can wash away the pollutants on the surface of the filter material and the inactivated, aged biofilm, which is beneficial to the renewal of the membrane and increases the activity of the biofilm.

When the hydraulic load continued to increase from 4 to 7 m/h, the average removal rate of COD_{Mn} decreased from 54.74 to 34.93%, and the average removal rate of ammonia nitrogen decreased from 66.91 to 58.60%. The shed biofilm causes an increase in the effluent COD_{Mn}, which is manifested by a decrease in the removal rate of COD_{Mn}. Although increasing hydraulic load can increase the rate of transport of organic matter and DO, it results in stronger flushing on the medium surface, reduces microbial biomass, shorter contact time between contaminants and biomass, and reduces removal rate [19]. Nitrifying bacteria are clearly at a disadvantage in competing for DO and nutrients in the absence of changes in gas to water ratio [20]. The growth rate of nitrifying bacteria is much lower than that of heterotrophic bacteria [21], so the overall activity decreases and the degradation ability of ammonia nitrogen decreases with the increase of hydraulic load. Increasing the hydraulic load leads to frequent backwashing, and washing away of the nitrifying bacteria is more likely, which results in a lower ammonia nitrogen removal rate.

The hydraulic load can affect the distribution of material concentration and the variation of the material along with the dielectric layer in the BAF. The optimal filtration rate of BAF may exist in the water treatment plant, which can effectively control the removal of major pollutants and the production of by-products [22]. This is one of the directions worthy of further study.

3.4. EFFECT OF IMPACT LOAD ON THE REMOVAL OF COD_{Mn} AND AMMONIA NITROGEN BY ASBAF

The impact load of the influent water is divided into COD_{Mn} load and ammonia nitrogen load. The effect of COD_{Mn} and ammonia nitrogen removal on ASBAF were

studied when subjected to COD_{Mn} shock load when ammonia nitrogen concentration is 3.86–4.23 mg/dm^3 and COD_{Mn} concentration is increased from 4.23 to 18.04 mg/dm^3. And the effect of COD_{Mn} and ammonia nitrogen removal on ASBAF were studied when subjected to ammonia nitrogen shock load when COD_{Mn} concentration is 6.94–8.31 mg/dm^3 and ammonia nitrogen concentration is increased from 2.34 to 18.73 mg/dm^3.

Effect of COD_{Mn} load on pollutant removal. Figure 5c shows the removal effect of ASBAF on COD_{Mn} and ammonia nitrogen when the concentration of COD_{Mn} increases from 4.23 to 18.04 mg/dm^3. The COD_{Mn} removal rate increases, and the ammonia nitrogen removal rate decreases as the COD_{Mn} load increases. ASBAF showed effective degradation under various COD_{Mn} rates [19]. When the concentration of COD_{Mn} increased from 4.23 to 18.04 mg/dm^3, the removal rate of COD_{Mn} increased from 27.36 to 39.24%, and the removal rate of ammonia nitrogen decreased from 81.32 to 63.38%. With the increase of COD_{Mn} load, the heterotrophic microorganisms in ASBAF obtain sufficient carbon source and enter a rapid proliferation period, so the removal rate of COD_{Mn} is gradually increased. Heterotrophic bacteria and nitrifying bacteria competed for living space and DO in the absence of changes in gas to water ratio and hydraulic loading conditions [20]. When the ammonia nitrogen concentration remained stable, the rate of proliferation of nitrifying bacteria also remained at a lower level. Therefore, the living space and DO that can be obtained by nitrifying bacteria are gradually occupied by heterotrophic bacteria, which reduces the removal rate of ammonia nitrogen, and begins autotrophic denitrification [16].

Effect of ammonia nitrogen impact load on pollutant removal. Figure 5d shows the effect of COD_{Mn} and ammonia nitrogen removal on ASBAF when subjected to ammonia nitrogen shock load when COD_{Mn} concentration is 6.94–8.31 mg/dm^3 and ammonia nitrogen concentration is increased from 2.34 to 18.73 mg/dm^3. This figure shows that the removal rate of COD_{Mn} is stable with the increase of ammonia nitrogen load, and the removal rate of ammonia nitrogen increases with the increase of ammonia nitrogen load. When the ammonia nitrogen concentration increased from 2.34 to 18.73 mg/dm^3, the removal rate of COD_{Mn} fluctuated within 31.33–40.49%, and the removal rate of ammonia nitrogen increased from 75.36 to 82.56%. With the increase of ammonia nitrogen load, the nitrifying bacteria in ASBAF obtained sufficient nutrients and entered the proliferative phase, so the removal rate of ammonia nitrogen gradually increased. Competition with heterotrophic bacteria for living space and DO is not intense because of the slower proliferation rate of nitrifying bacteria [21]. Therefore, nitrifying bacteria and heterotrophic bacteria can coexist in the ASBAF system relatively smoothly. Macroscopically, the removal rate of COD_{Mn} remained stable overall, and the removal rate of ammonia nitrogen gradually increased.

Besides, there are dynamic adsorption and bioconversion processes on the AS filter. When the adsorption on the AS filter material is saturated, the organic matter and ammonia nitrogen adsorbed by the biofilm on the filter material undergo bioconversion, so

that the adsorption site is vacated. At this time, the biofilm can adsorb organic matter and ammonia nitrogen [23], so that the biofilm can be regenerated. When the influent impact load is large, even if the proliferation rate of heterotrophic bacteria and nitrifying bacteria cannot meet the degradation requirements, AS filter material can also adsorb more organic matter and ammonia nitrogen in the water, thus strengthening the ability of ASBAF to resist impact load. When the influent impact load is small, the organic matter and ammonia nitrogen adsorbed on the AS filter material can be analyzed and bioconverted, so that the effluent water quality is guaranteed [23].

3.5. EFFECT OF BACKWASHING ON THE REMOVAL OF COD_{Mn} AND AMMONIA NITROGEN BY ASBAF

Figure 6a shows the removal of contaminants by ASBAF before and after backwashing. The influent COD_{Mn} and suspended solids (SS) concentration are the main factors affecting the backwashing strength and backwashing cycle. Therefore, the COD_{Mn} concentration of the influent was 8.38 mg/dm^3, and the ammonia nitrogen concentration was 3.61 mg/dm^3 before and after the backwashing. The removal rate of COD_{Mn} was improved before and after backwashing, and the removal rate of ammonia nitrogen remained stable. Two hours before backwashing, the removal rate of COD_{Mn}

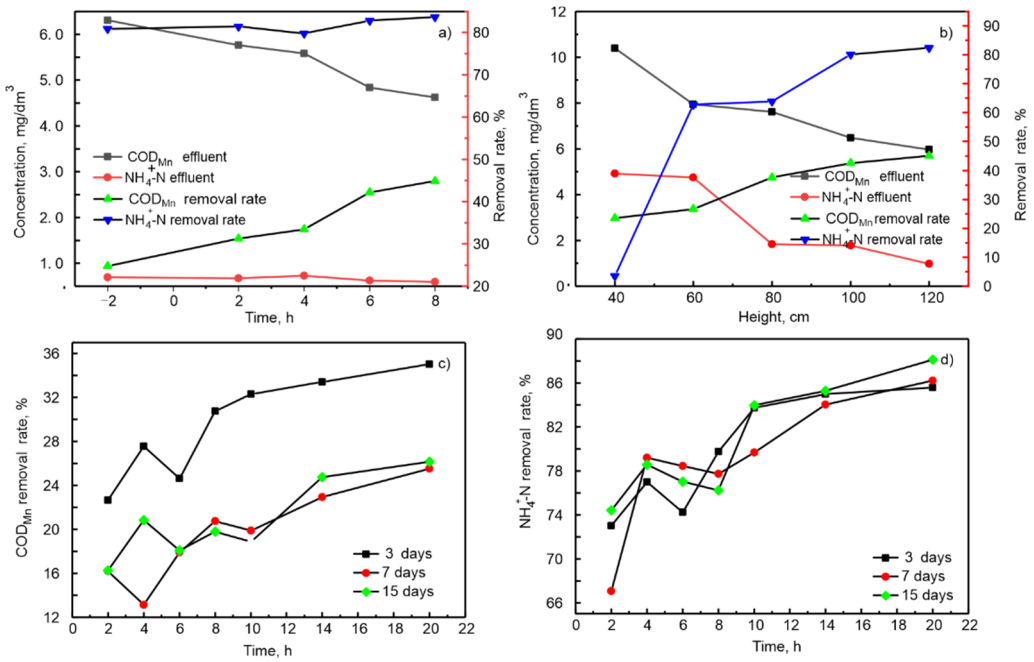

Fig. 6. Time dependences of load concentration for various values of backwashing (a), height (b), filter closing time on COD removal (c), and nitrogen removal (d)

was only 24.7%, and the removal rate of ammonia nitrogen was 80.89%. After backwashing, the removal rate of COD_{Mn} increased from 31.26 to 44.87%, and the removal rate of ammonia nitrogen only increased from 81.44 to 83.66%. The ASBAF effluent water quality fluctuated little during the normal operation period. And after two hours after backwashing, the treatment effect became stable. Before backwashing, the filter layer traps excessive suspended particles and flocs, causing blockage of the filter layer, which adversely affects the degradation process of the organism. After backwashing, the clogging of the filter layer was greatly alleviated, and the mass transfer efficiency of the filter material was improved. The aged biofilm of the filter material was discharged into the ASBAF system together with the flocs by backwashing [24], which greatly increased the activity of the biofilm. Therefore, after backwashing, the removal rate of COD_{Mn} was substantially improved.

The biofilm formed by nitrifying bacteria with a long generation time was relatively dense, and the shear resistance against backwashing was relatively strong [21]. Therefore, the faster growing heterotrophic bacteria and the suspended solids adsorbed by the biofilm are easily washed up to the top of the filter column by backwashing, while most of the nitrifying biofilm remains attached to the surface of the filter. After backwashing, the microbial community in the upper part of BAF substantially increased, while the lower microbial community decreased [24]. Therefore, there was almost no effect on the performance of ASBAF to remove ammonia nitrogen after backwashing.

3.6. EFFECT OF THE HEIGHT OF FILTER LAYER ON THE REMOVAL OF COD_{Mn} AND AMMONIA NITROGEN BY ASBAF

Figure 6b illustrates that increased height of the water intake corresponds to higher removal rates of COD_{Mn} and ammonia nitrogen change from 23.53 and 45.08% to 3.54 and 82.45%, respectively. As the height of the filter layer changes, variations in DO and substrate concentration can alter the type and amount of microorganisms, resulting in differences in the thickness of the biofilm [22]. When the height of the water intake is 40 cm, the removal rate of COD_{Mn} is only 23.53%, but the removal amount of COD_{Mn} is 2.44 mg/dm^3. The removal of COD_{Mn} from 0 to 40 cm is best compared to the removal for other heights. At the bottom of the ASBAF, the heterotrophic bacteria multiply rapidly because they can obtain sufficient nutrients and DO in this section. Therefore, organic matter can be rapidly degraded by microorganisms. Although the total removal rate of COD_{Mn} is increased as the height is increased, the amount of COD_{Mn} degraded by the same volume of the filter material decreases. Because as the height of the filter layer increases, the COD_{Mn} concentration and DO concentration gradually decrease, the number of aerobic bacteria on the surface of the filter material decreases, and the thickness of the biofilm decreases [18]. The substrate concentration at these filter layers is a major factor limiting the rate of COD_{Mn} degradation. The surface porosity of the AS filter material also enhances the adsorption of COD_{Mn}. At the heights of 60, 80, 100,

and 120 cm, the total removal rate of COD_{Mn} steadily increased and was maximized at 120 cm.

ASBAF has an extremely low removal rate of ammonia nitrogen at a height of 40 cm. Heterotrophic bacteria become dominant bacteria because the concentration of organic matter at the bottom of the ASBAF is higher than the concentration of ammonia nitrogen. Nitrifying bacteria were in a disadvantaged position because of the competitive effect on the living space and DO concentration, so there was a low removal rate of ammonia nitrogen. The organic nitrogen in the influent is converted to ammonia nitrogen by the amination reaction at a relatively low DO concentration so that the ammonia nitrogen removal rate at the bottom of the ASBAF is low [16]. At a height of 60 cm, the ammonia nitrogen removal rate increased to 62.76%. At this time, most of the organic nitrogen in the influent water was converted into ammonia nitrogen, and the competition is alleviated between the heterotrophic bacteria and the nitrifying bacteria for the living space and DO. Therefore, the removal rate of ammonia nitrogen was greatly improved. At 80, 100, and 120 cm, DO is relatively sufficient, and the total removal rate of ammonia nitrogen continues to increase.

3.7. EFFECT OF ASBAF CLOSED ON THE REMOVAL OF COD_{Mn} AND AMMONIA NITROGEN BY ASBAF

It can be seen from Figs. 7a–c that after ASBAF restarts, the removal rates of COD_{Mn} and ammonia nitrogen increase with the increase of filter operation time.

However, after the filter was closed for three days, seven days, and fifteen days, the COD_{Mn} removal rate was laterally compared in Fig. 6c, which shows that the removal of the filter for three days does not have a substantial effect on the removal of COD_{Mn}. After restarting for four hours, ASBAF resulted in a noticeable film-hanging effect. After six hours of restart, the COD_{Mn} removal rate reached a relatively stable value and normal level before the ASBAF shuts down. The filter was restarted after seven days and fifteen days, and the COD_{Mn} removal rates at the initial operation were at low levels of 16.22 and 16.28%, respectively. After 20 hours of normal operation, the ASBAF closed for seven days and fifteen days resulting in a noticeable film-hanging effect, and the removal rate of COD_{Mn} reached 25.52 and 26.17%, respectively. The biofilm on the surface of the filter material can trap some organic matter.

After the filter is closed, these microorganisms can continue to use these organic substances, which can delay the arrival of microbial decline [25]. Therefore, the short-time closure of the filter does not have a substantial effect on the removal of COD_{Mn}. When the organic matter adsorbed on the biofilm and the AS filter material is completely degraded by the heterotrophic bacteria, the heterotrophic biofilm begins to enter the endogenous respiration period, and the number of heterotrophic bacteria gradually decreases. Therefore, the cultivation of the heterotrophic bacteria needs to be repeated because COD_{Mn} removal is limited after a long period of filter shut down.

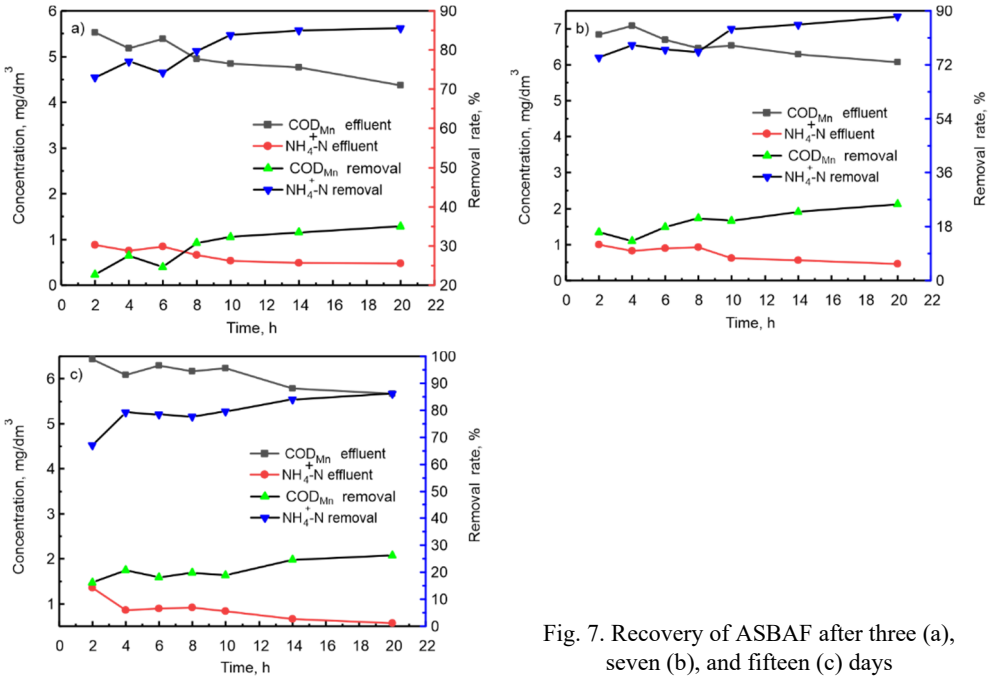

Fig. 7. Recovery of ASBAF after three (a), seven (b), and fifteen (c) days

In Figure 6d, the ammonia nitrogen removal rates after the filter was turned off for three, seven, and fifteen days have been shown. Removal of the ammonia nitrogen by the restart of the filter seems to be independent of time. At the beginning of the restart of the filter tank, the removal rate of ammonia nitrogen can still be about 70%. By the 14th hour, it has recovered nearly to the level before the shutdown, and at the 20th hour it has completely recovered to the level before the shutdown because the growth cycle of nitrifying bacteria is slower than that of heterotrophic bacteria, but the life cycle is longer, the dormancy period can be up to two years [21]. Moreover, the filter material has an adsorption effect on ammonia nitrogen, and the proliferation of nitrifying bacteria is slow, so the number of nitrifying bacteria is hardly affected by the closure of the filter [23].

3.8. KINETICS OF DEGRADATION OF ORGANIC MATTER

Equation (10) is a matrix degradation kinetic model related to such factors as the maturity of the biofilm at the specific reaction time, reaction environment, filter characteristics, influent water quality, active biomass, reactor size, and the hydraulic load. In this test, the size of the test device has been determined, the filter material and the reaction environment are unchanged, and the biofilm is stable in a steady state, so the specific reaction time and the amount of biological activity under each condition are determined. Therefore, the degradation rate of organic matter in the reactor water in the

case of stable influent water quality is only related to the height of the filter material and the hydraulic load

$$S = S_0 \exp\left(-\frac{KA}{Q}h\right) = S_0 \exp\left(-\frac{KA}{uA}h\right) = S_0 \exp\left(-\frac{K}{u}h\right) = S_0 \exp\left(K_u h\right) \quad (11)$$

where S and S_0 are the effluent and influent matter concentrations, respectively, u – the hydraulic load, K_u – the kinetic parameter associated with hydraulic loading.

In the logarithmic form, we obtain

$$\ln\left(\frac{S}{S_0}\right) = K_u h \quad (12)$$

K_u may be determined by fitting the straight line of $\ln(S/S_0)$ in function of h. When the hydraulic load is low, the nutrients available to microorganisms in ASBAF oxidizing bacteria are insufficient. Therefore, the ASBAF organic matter degradation model needs to re-add parameters related to microbial abundance. The subsequent parameter determinations were carried out under a hydraulic load greater than 4 m/h. Water output values at different filter heights under the hydraulic load of 4 m/h are given in Table 2. Gas to water ratio used in the test was 2:1.

Table 2

Kinetic test data of different heights

h, cm	0	40	60	80	100	120
S, mg/dm^3	13.59	10.39	7.94	7.61	6.48	5.97

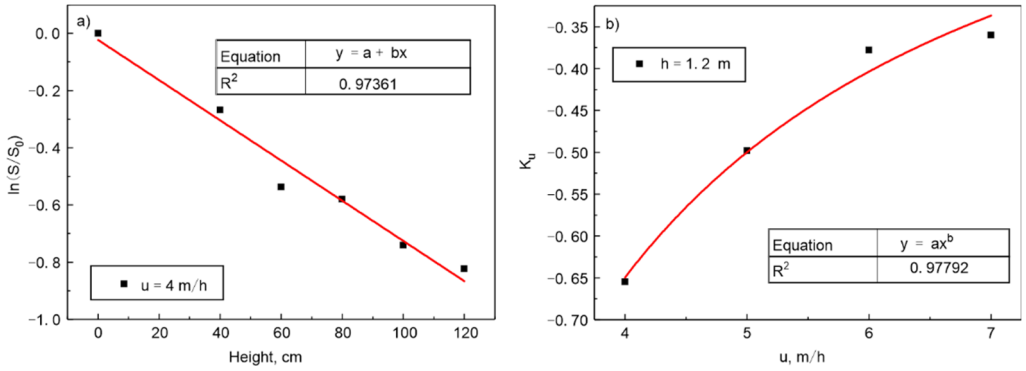

Fig. 8. Curve fitting of organic matter degradation model (a), and K_u (b) to hydraulic load u

As can be seen in Fig. 8a, the coefficient of determination R^2 is 0.97361, indicating that equation (11) may be used to describe the degradation of organic matter on ASBAF.

The test to determine K values was carried out at the height of 120 cm, gas to water ratio 2:1. The water outputs at various hydraulic loads are shown in Table 3.

Table 3

Kinetic test data for hydraulic load

Concentration	u [m/h]			
	4	5	6	7
S_0, mg/dm^3	8.49	7.67	7.50	7.30
S, mg/dm^3	3.87	4.22	4.77	4.75
$\ln(S/S_0)$	–0.786	–0.598	–0.453	–0.430
K_u (eq. (12))	–0.6550	–0.4983	–0.3775	–0.3583

The equation describing the dependence of K_u on u (Fig. 8b) has been determined ($R^2 = 0.97792$). It may be used to describe indicating that Equation 13 is used to model the kinetics of degradation of organic matter on ASBAF

$$K_u = -3.1142u^{-1.17475} \tag{13}$$

By substituting equation (13) into (11), an equation describing kinetics of complete ASBAF degradation can be obtained

$$S = S_0 \exp\left(-3.1142u^{-1.17475}h\right) \tag{14}$$

The COD_{Mn} concentration in the ASBAF effluent under optimal operating conditions was used to verify equation (14). In Table 4, the concentrations of organic substrate – influent (S_0), experimental (S_1) and calculated from the model equation (S_2) are given. The simulation results are lower than the experimental ones, but the relative error does not exceed 15% (Table 4). Therefore, we conclude that the model formula roughly reflects the degradation process of organic matter under optimal operating conditions. The experimental results are different from the calculated results, which may be due to the mass transfer of the material in the filter, the nature of the filter material, the presence of aerobic, anoxic and anaerobic reactions in the biofilm or filter.

Table 4

Concentrations of organic substrate

Concentration	u [m/h]			
	4	5	6	7
S_0, mg/dm^3	10.53	9.42	11.36	10.87
S_1, mg/dm^3	4.87	4.69	6.37	6.84
S_2, mg/dm^3	5.05	5.35	7.20	7.43

4. CONCLUSION

Attapulgite suspended (AS) is a high-quality filter material, easy to prepare and inexpensive. It floats on the water, which helps to optimize hydraulic conditions and reduce costs. When the hydraulic load is 4 m/h and the gas to water ratio is 2:1, a biological aerated filter with attapulgite suspended filter material (ASBAF) can stably treat micropolluted water into a qualified drinking source water. Besides ASBAF has a strong ability to resist impact load. Different operating conditions have a greater impact on ASBAF processing performance. Biomass is the main factor for ASBAF to remove pollutants, and different operating conditions affect the biomass inside ASBAF. Therefore, the selection of operating conditions is very important. A complete organic matter degradation equation for ASBAF has been derived. When ASBAF is applied to practical engineering, it has important reference significance. In general, ASBAF has excellent performance and lower operating cost in the treatment of micropolluted water, showing the potential of being widely used in the pretreatment of micropolluted water.

ACKNOWLEDGEMENTS

The authors express their sincere gratitude to the National Natural Science Foundation of China (51608272) and the Science and Technology Project of Jiangsu Provincial Department of Housing and Urban-Rural Development (2017ZD055).

REFERENCES

[1] HICK J.L., BIDDINGER P.D., N*ovel coronavirus and old lessons – preparing the health system for the pandemic*, New Eng. J. Med., 2020, 382 (20), e55(1–3).
[2] LEGINOWICZ M., SIEDLECKA A., PIEKARSKA K., *Biodiversity and antibiotic resistance of bacteria isolated from tap water in Wrocław, Poland*, Environ. Prot. Eng., 2018, 44 (4), 85–98.
[3] CHEN Z., YU D., HE S., YE H., ZHANG L., WEN Y., ZHANG W., SHU L., CHEN S., *Prevalence of antibiotic-resistant Escherichia coli in drinking water sources in Hangzhou city*, Front. Microbiol., 2017, 8, 1133.
[4] CAO S., JING Z., YUAN P., WANG Y., WANG Y., *Performance of constructed wetlands with different substrates for the treated effluent from municipal sewage plants*, J. Water Reuse Des., 2019, 9 (4), 452–462.
[5] CAO S., JING Z., WANG Z., *The coordination between macrophytes and fly ash ceramsite in compound vertical flow constructed wetland*, Fresen. Environ. Bull., 2019, 28 (12A), 9935–9943.
[6] XIE T., JING Z., HU J., YUAN P., LIU Y., CAO S., *Degradation of nitrobenzene-containing wastewater by a microbial-fuel-cell-coupled constructed wetland*, Ecol. Eng., 2018, 112, 65–71.
[7] HWANG C., WENG C., *Key factors contributing to simultaneous nitrification-denitrification in a biological aerated filter system using oyster shell medium*, Environ. Prot. Eng., 2017, 43 (1), 75–86.
[8] WANG Z., ZHONG M., WAN J., XU G., LIU Y., *Development of attapulgite composite ceramsite/quartz sand double-layer biofilter for micropolluted drinking source water purification*, Int. J. Environ. Sci. Technol., 2016, 13 (3), 825–834.
[9] WANG Z., WANG Z., CHEN L., LIN Z., LIU Y., LIU Y., *Using an attapulgite-activated carbon composite ceramsite biofilter to remove dibutyl phthalate from source water*, Pol. J. Environ. Stud., 2018, 27 (2), 897–901.

[10] Committee of Water and Wastewater Monitoring and Analysis Methods of the State Environmental Protection Administration, *Water and wastewater monitoring and analysis methods*, China Environmental Science Press, Beijing 2002.
[11] LEVENSPIEL O., *Chemical reaction engineering: an introduction to the design of chemical reactors*, Wiley, New York 1962.
[12] KARGI F., *Reinterpretation of the logistic equation for batch microbial growth in relation to Monod kinetics*, Lett. Appl. Microbiol., 2009, 48 (4), 398–401.
[13] LIU Y., CAPDEVILLE B., *Specific activity of nitrifying biofilm in water nitrification process*, Water Res., 1996, 30 (7), 1645–1650.
[14] CHEN H., LIU Y., X21-4021U X., SUN M., JIANG M., XUE G., LI X., LIU Z., *How does iron facilitate the aerated biofilter for tertiary simultaneous nutrient and refractory organics removal from real dyeing wastewater?*, Water Res., 2019, 148, 344–358.
[15] LIU T., QUAN X., LI D., *Evaluations of biofilm thickness and dissolved oxygen on single stage anammox process in an up-flow biological aerated filter*, Biochem. Eng. J., 2017, 119, 20–26.
[16] KIM D.J., KIM Y., *Effect of aeration on nitrous oxide (N_2O) emission from nitrogen-removing sequencing batch reactors*, J. Microbiol. Biotechnol., 2013, 23 (1), 99–105.
[17] ZHANG Q., WANG C., JIANG L., QI J., WANG J., HE X., *Impact of dissolved oxygen on the microbial community structure of an intermittent biological aerated filter (IBAF) and the removal efficiency of gasification wastewater*, Bioresour. Technol., 2018, 255, 198–204.
[18] YUE X., YU G., LU Y., LIU Z., LI Q., TANG J., LIU J., *Effect of dissolved oxygen on nitrogen removal and the microbial community of the completely autotrophic nitrogen removal over nitrite process in a submerged aerated biological filter*, Bioresour. Technol., 2018, 254, 67–74.
[19] PRIYA V.S., PHILIP L., *Treatment of volatile organic compounds in pharmaceutical wastewater using submerged aerated biological filter*, Chem. Eng. J., 2015, 266, 309–319.
[20] CASTELLANO-HINOJOSA A., MAZA-MARQUEZ P., MELERO-RUBIO Y., GONZALEZ-LOPEZ J., RODELAS B., *Linking nitrous oxide emissions to population dynamics of nitrifying and denitrifying prokaryotes in four full-scale wastewater treatment plants*, Chemosphere, 2018, 200, 57–66.
[21] YOUNG B., DELATOLLA R., ABUJAMEL T., KENNEDY K., LAFLAMME E., STINTZI A., *Rapid start-up of nitrifying MBBRS at low temperatures: Nitrification, biofilm response and microbiome analysis*, Bioproc. Biosyst. Eng., 2017, 40 (5), 731–739.
[22] MA T., CHEN Y., KANG J., GAO X., GUO J., FANG F., ZHANG X., *Influence of filtration velocity on DON variation in BAF for micropolluted surface water treatment*, Environ. Sci. Poll. Res., 2016, 23 (23), 23415–23421.
[23] FENG Y., YU Y., QIU L.P., YANG Y., LI Z., LI M., FAN L., GUO Y., *Impact of sorption functional media (SFM) from zeolite tailings on the removal of ammonia nitrogen in a biological aerated filter*, J. Ind. Eng. Chem., 2015, 21, 704–710.
[24] FENG Y., LI X., SONG T., FAN L., YU Y., QI J., WANG X., *Effect of backwashing on the microbial community structure and composition of a three dimensional particle electrode coupled with biological aerated filter reactor (TDE-BAF)*, Ecol. Eng., 2017, 101, 21–27.
[25] SHI W., DUAN Y., YI X., WANG S., SUN N., MA C., *Biological removal of nitrogen by a membrane bioreactor-attapulgite clay system in treating polluted water*, Desalination, 2013, 317, 41–47.